The potential of Ojo de Valjunquera cave (NE of Iberia) sediments for paleoflood reconstructions

El potencial de los sedimentos de la cueva del Ojo de Valjunquera (NE de Iberia) para la reconstrucción de paleoinundaciones

Bartolomé, M. [(1)*], Benito, G. [(1)], Luetscher, M. [(2)], Badules-Iglesias, J. [(3)], Pérez-Villar, G. [(3)], Edwards, R.L. [(4)], Moreno A. [(5)]

(1) Departamento de Geología, Museo Nacional de Ciencias Naturales-CSIC. C/José Gutiérrez Abascal 2, 28006, Madrid, España. mbart@mncn.csic.es
(2) Swiss Institute for Speleology and Karst Studies (SISKA). Rue de la Serre 68 2301. La Chaux-de-Fonds. Switzerland
(3) Departamento de Ciencias de la Tierra, Universidad de Zaragoza. C/ Pedro Cerbuna, 12, 50009, Zaragoza, España
(4) Isotope Geochemistry Laboratory, School of Earth and Environmental Sciences, University of Minnesota, John T. Tate Hall, 116 Church Street SE, Minneapolis, MN 55455, USA
(5) Departamento de Procesos Geoambientales y Cambio Global, Instituto Pirenaico de Ecología-CSIC. Avda/ Montañana, 1005, 50059, Zaragoza, España

Abstract

Speleothems and detrital deposits in caves are excellent archives of past flood events but are still poorly exploited. In this study we evaluate, the potential of the Ojo de Valjunquera cave (Zaragoza, NE Spain) for the study of past floods based on geomorphological, topographical, hydrological, and chronological data. The cave comprises two subhorizontal levels. The lower level consists of a main horizontal conduit including six siphons. This level is connected to the upper one by shafts and ramps. That situation, together with the constrictions of the gallery in the lower level, favours the water rise during rainfall events. The upper level is characterized by a larger presence of speleothems and detrital sequences compared to the lower level. Current observations indicate that water can rise by ~9 m in some cave sectors during rainfall episodes >60 mm, although the hydraulic head rise is not homogeneous along the cave, depending on the section's morphology. The stalagmites and detrital sequences hosted in the upper gallery most likely contain evidence of extreme events of rainfall. However, geomorphological and sedimentological evidences also suggest that the cave outlet could have been blocked in the past by sediments, favouring the water rise to high places usually not affected by regular floods. The detrital sequences located in lower positions with respect to the cave entrance show a higher proportion of sandy sediments than those located in the higher sectors related to the water energy during the flood. Stalagmites show clean carbonate alternating with well-defined detrital layers. These detrital layers vary in thickness: the thinner ones are related to small floods, whereas the thicker ones are connected to large floods. Two important

historical floods (1709 and 1755 CE) occurred in the area that coincide with distinct detrital layers recorded in the stalagmites. All these observations suggest that Ojo de Valjunquera cave contains an important paleoflood archive based on speleothems and detrital deposits during the Holocene.

Key words: paleoflood; stalagmites; Iberian Range; Moncayo; cave sediments.

Resumen

Los espeleotemas y secuencias detríticas de las cuevas contienen registros detallados de inundaciones del pasado, aunque han sido poco utilizadas para este fin. En este trabajo evaluamos, en base a observaciones geomorfológicas, topográficas, hidrológicas y cronológicas, el potencial e idoneidad de la cueva Ojo de Valjunquera (Zaragoza, NE de España) para el estudio de inundaciones pasadas. La cueva tiene dos niveles pseudo-horizontales. El nivel inferior presenta un río y seis sifones. Este nivel está conectado al superior mediante pozos y rampas. Esa situación, además de las constricciones en la galería inferior, favorecen la subida del agua durante importantes eventos de lluvia. El nivel superior presenta una mayor cantidad de espeleotemas y secuencias detríticas que el nivel inferior. Las observaciones actuales indican que el agua puede subir aproximadamente 9 m en algunos sectores de la cueva durante episodios de precipitaciones acumuladas superiores a 60 mm. Sin embargo, la subida del nivel de agua parece no ser homogénea a lo largo de la cueva, dependiendo de la morfología de las diferentes secciones. De acuerdo a estas observaciones, las estalagmitas y secuencias detríticas registradas en la galería superior se asocian a eventos extremos de lluvia. Por otro lado, las evidencias geomorfológicas y sedimentológicas también sugieren que la salida de la cueva pudo estar bloqueada en el pasado por sedimentos, favoreciendo fácilmente el ascenso del agua durante inundaciones regulares, a zonas altas no inundadas frecuentemente. Las secuencias detríticas ubicadas en posiciones más bajas respecto a la entrada de la cueva muestran un mayor porcentaje de arena que las ubicadas en los sectores más altos, en relación a la energía de las aguas durante la crecida. Las estalagmitas presentan una alternancia de carbonato limpio y capas detríticas bien definidas. Las capas detríticas comprenden capas delgadas y gruesas, que parecen estar en relación con pequeñas y grandes inundaciones respectivamente. Dos importantes inundaciones históricas (1709 y 1755 DC) que ocurrieron en el área, parecen estar registradas en las estalagmitas. Todas estas observaciones hacen del Ojo de Valjunquera una cueva idónea y con alto potencial para la reconstrucción de paleoinundaciones y lluvias extremas a partir de espeleotemas y depósitos detríticos durante el Holoceno.

Palabras clave: paleoinundaciones; estalagmitas; Cordillera Ibérica; Moncayo; sedimentos de cuevas.

1. Introduction

A recent European-wide study has identified the last three decades as one of the most flood-rich periods of the last 500 years in Europe (Blöschl *et al.*, 2020). This study shows that while in the past flood-rich periods occurred during cooler episodes, the recent recurrence of floods occurs in conditions of global warming. Perhaps more importantly, it shows the relevance of atmospheric processes that generate floods beyond the prevailing temperature conditions, and the paramount interest of analysing extreme events over extended climatic cycles.

The reconstruction of flood events at a long-term scale can only be achieved by studying the geological paleoflood records (Wilhelm *et al.*, 2019). The characterization of past floods events in terms of frequency and intensity can help us to understand the flood variability in space and time and improve predictions for the nearby future. Several studies with that goal point to changes in atmospheric circulation pattern as the main cause controlling the frequency of large floods during the Holocene (Thorndycraft and Benito, 2005; Benito *et al.*, 2008, 2015). The most common geological archives to characterize the frequency of past extreme events comprise lake and fluvial

En prensa

In press

sediments (Arnaud, 2005; Corella *et al.*, 2016; Benito *et al.*, 2015). Only recently, detritus trapped in speleothems have been used as natural paleoflood archives (Denniston *et al.*, 2015; Denniston and Luetscher, 2017; González-Lemos *et al.*, 2015a, 2015b). The number of studies that use speleothems as paleoflood records is limited worldwide, with only three studies located in the Iberian Peninsula (Gázquez *et al.*, 2014; González-Lemos *et al.*, 2015a, 2015b). Thus, the potential of speleothems, together with cave detrital sequences, as a paleoflood archive, is still unexploited.

Karst systems have a complex response to water input mostly based on thresholds and therefore, do neither show a linear nor gradual response. A singular risk affects touristic caves and/or speleological explorations when an abrupt increase in cave-water levels may cause the loss of human lives. Recently, problems associated with cave flooding have appeared in the news becoming important public concerns. Some examples include the rescue of children trapped in Tham Luang cave (2018; Thailand), or the speleologists that remained several days in a cave in Teruel province (2018; Spain). Understanding the hydraulic response of a cave system is thus of fundamental interest.

During a flood in a cave, the water level may rise by several tens to hundreds of meters with respect to the hydrological base level (e.g Denniston and Luetscher, 2017). Speleothems situated next to a cave stream can record ordinary floods by incorporating detrital sediment layers transported during the flood. In contrast, those located far from these cave passages or in upper cave levels may only record extraordinary floods. When the energy of the stream decreases, a fine sediment layer comprising silts and sands may coat (sometimes visible but not always) the speleothem surfaces (Denniston and Luetscher, 2017; González-Lemos *et al.*, 2015a, 2015b). The active precipitation of calcite traps these detrital layers inside the speleothems. The speleothems can then be accurately dated

by U disintegration series (^{238}U-^{234}U-^{230}Th), although the incorporation of detrital particles may significantly alter the age precision. Alternatively, and providing the dead carbon fraction is known, radiocarbon techniques can be used to date speleothems with high detrital contamination (e.g. González-Lemos *et al.*, 2015b). Speleothems with high growth rates (≥200 μm a^{-1}) subjected to flood recurrences of ≥10 years are among the best natural archives for long-term paleoflood reconstructions (Wilhelm *et al.*, 2019).

The aim of this research is to evaluate the potential of the Ojo de Valjuquera cave (OdV cave henceforth) for the reconstruction of paleofloods based on preliminary geomorphological, topographical, hydrological and chronological cave observations. This particular cave is selected since it is located in a region prone to floods with historical damages. Additionally, the instrumental record of precipitation is too short in the area to relate the floods with rainfall amounts. Speleothems and detrital deposits for that cave provide the opportunity to evaluate their suitability as paleoflood archives.

2. Study site

The OdV cave (41° 45 '20.64" N; 1° 37' 57.84" W, ~700 m asl) is located in the transition zone between the highlands of the Iberian Range and the Ebro Basin (Fig. 1A), next to the Moncayo Natural Park whose maximum elevation is the Moncayo peak (2314 m a.s.l). The position and the high elevation of Moncayo with respect to the surrounding arid/semi-arid lowlands, provides local/regional climate particularities. The Moncayo Massif, ~16 km long and NW-SE orientation (Fig. 1A), represents an orographic barrier to Atlantic fronts during winter and spring, that favours the formation of storms. The climate of the area is characterized by warm and dry summers and cold and dry winters. The mean annual temperature is ~11.4 °C, while the maximum and minimum monthly mean temperatures vary between ~20.5°C (July) and ~3.6 °C
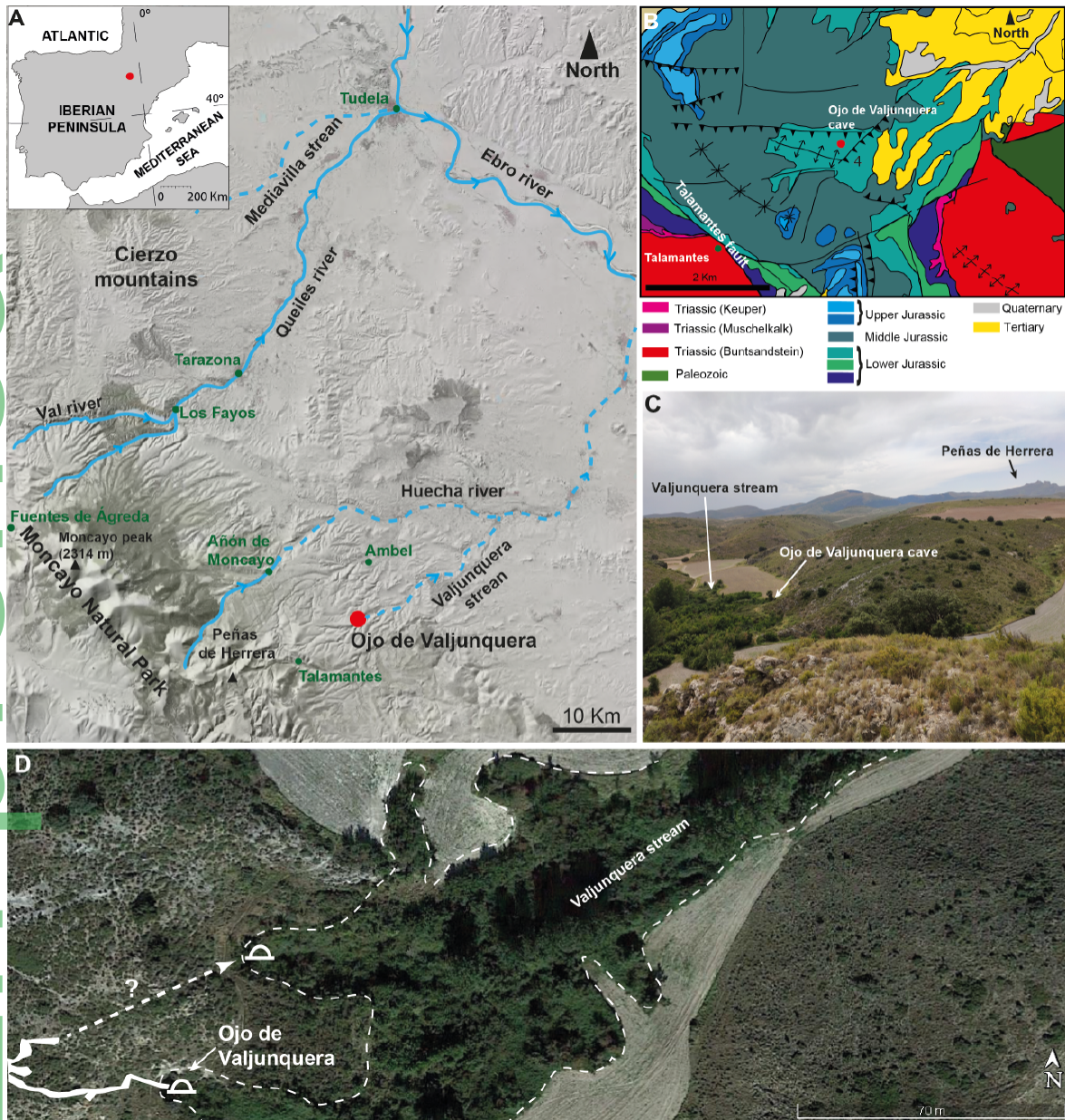
Figure 1. (A) Location of Ojo de Valjunquera cave and the main rivers. Continuous blue lines indicate perennial rivers and discontinuous ones show ephemeral streams. (B) Synthetic geological map of the studied area. (C) View of cave surroundings. White arrows indicate the Valjunquera stream and the upper and lower cave entrances. (D) Aerial view of Valjunquera stream and the location of cave entrances (©Google Earth). White arrows indicate the Valjunquera stream and cave entrance.

Figura 1. (A) Localización de la Cueva del Ojo de Valjunquera y los principales ríos. Las líneas azules representan ríos perennes, y las discontinuas corresponden a corrientes efímeras. (B) Mapa geológico sintético de la zona de estudio. (C) Vista de los alrededores de la cueva. Las flechas blancas indican el barranco de Valjunquera y las entradas superior e inferior de la cueva. (D). Vista aérea del barranco de Valjunquera y localización de las entradas de la cueva (©Google Earth). Las flechas blancas indican el barranco de Valjunquera y la entrada de la cueva.

(January), respectively. The annual rainfall is ~600 mm, mostly concentrated during spring and autumn (Cuadrat *et al*., 2008). The cave is placed in the meso-Mediterranean bioclimatic belt, characterized by Mediterranean oak communities, with an open understory composed of *Salvia rosmarinus*, *Lavandula latifolia*, *Juniperus oxycedrus* and *Genista rigidissima*, among others, similar to those described by Longares (2004). Hydrological runoff observed on the northern side of the Moncayo massif, and from the West to East, comprises the rivers Val, Queiles, and Huecha (Fig. 1A). Such as in other Iberian Range rivers (Sancho *et al*., 2015), Val and Queiles rivers had a moderate tufa development during the Holocene (Aranbarri *et al*., 2016). Val and Queiles are regulated by reservoirs, hydro-electrical plants and water derivations for irrigation, while Huecha River preserves a semi-natural regime. The flow of Huecha River infiltrates downstream of Añón de Moncayo village, and only during intense rainfall episodes the water circulates in the lower reach of the river.

Geologically, the highest summits of the Moncayo Massif are formed mainly by Triassic (Buntsandstein) sediments. Well-karstified carbonate outcrops appear at low altitudes, surrounding the Moncayo, and are in contact with the Buntsandstein siliciclastic materials along the Talamantes fault (Fig. 1B). Tertiary materials formed by polymictic sands and conglomerates outcrop downstream to the cave. The cave opens in a stratigraphic series of limestone and dolostones Jurassic in age (Fig. 1B). The landscape around the cave is characterized by rolling hills (Fig. 1C). The slope deposits reach to the bottom of the valleys with colluvium of up to ~4 m in thickness. Small creeks, escarps, and fluvial terraces are also ubiquitous geomorphological landforms. The OdV cave is a seasonal spring that feeds the Valjunquera stream. The Valjunquera stream drains the area, and flows in an approximate SW-NE direction towards Ambel village (Fig. 1A) to flow out into the Río Huecha which joins the Ebro River further downstream. In origin, the cave could have had two entrances (Fig. 1D) located at

similar elevation. Nowadays, the gallery located downstream of OdV cave is completely blocked by sediments. Five hundred meters from OdV, some springs and a borehole were captured and derived for drinking water to Ambel village in the seventies.

Hydrologically, the Talamantes fault plays an important role in the hydrogeology of the Moncayo Massif. Many streams infiltrate at the contact between the impermeable Buntsandstein and the Lower Jurassic carbonate (LIAS aquifer) (San Román *et al*., 1989). In the Añón de Moncayo floodplain, the general piezometric level is more than 100 m deep (San Román *et al*., 1989) as suggested by a borehole (227 m deep, 2006 year) located ~3 km downstream from the cave that indicates a water level 143 m below the surface (CHEBRO, 2006).

3. Material and methods

This multidisciplinary study was focused on cave geomorphology, chronology, stratigraphy, and sedimentological features of the main clastic deposits as well as on morphostratigraphic relations between the different internal cave deposits. Simplified geomorphological features were surveyed on an earlier cave topography (Gisbert and Pastor, 2006). Inside the cave, two trenches were dug in the thickest deposits for sedimentological descriptions. Rainfalls in the area and the river flow of Huecha and Queiles Rivers were evaluated using the pluviometric data and gauging stations derived from Confederación Hidrográfica del Ebro (CHEBRO) meteorological station network. The stations are located at 7.5 km (Añón de Moncayo), 18 km (Los Fayos) and 24 km (Fuentes de Ágreda) from the cave.

Four stalagmites were sampled *in situ* to evaluate the preservation of detrital layers within the carbonate speleothems. The stalagmites were cut parallel to their growth axis and polished with a diamond disc. The basal age of two modern-looking stalagmites was deter-

Table 1. U/Th-series data and ages of stalagmites considering 2σ error. U decay constants: λ_{238} = 1.55125x10^{-10} (Jaffey *et al*., 1971) and λ_{234} = 2.82206x10^{-6} (Cheng *et al*., 2013). Th decay constant: λ_{230} = 9.1705x10^{-6} (Cheng *et al*., 2013). Corrected ^{230}Th ages assume the initial ^{230}Th/^{232}Th atomic ratio of 4.4 ±2.2 x10^{-6}. Those are the values for a material at secular equilibrium with the bulk earth ^{232}Th/^{238}U value of 3.8. The errors are arbitrarily assumed to be 50%. * δ^{234}U = ([^{234}U/^{238}U] $_{activity}$ - 1) x 1000. ** δ^{234}U$_{initial}$ was calculated based on ^{230}Th age (T). i.e. δ^{234}U$_{initial}$ = δ^{234}U$_{measured}$ x e$^{λ.234xT}$.

*Tabla 1. Datos de U/Th y edades de las estalagmitas considerando un error 2σ. La constante de desintegración del U es: λ_{238} = 1,55125x10^{-10} (Jaffey et al., 1971) y λ_{234} = 2,82206x10^{-6} (Cheng et al., 2013). La constante de desintegración del Th es: λ_{230} = 9,1705x10^{-6} (Cheng et al., 2013). ^{230}Th/^{232}Th de 4,4 ±2,2 x10^{-6}. Esos son los valores para el Material en equilibrio secular, con un valor ^{232}Th/^{238}U de 3,8. Los errores se asumen, arbitrariamente, como del 50%. * δ^{234}U = ([^{234}U/^{238}U] $_{actividad}$ - 1) x 1000. ** δ^{234}U$_{inicial}$ fue calculado con base en ^{230}Th age (T). i.e. δ^{234}U$_{inicial}$ = δ^{234}U$_{medido}$ x e$^{λ.234xT}$.*

Sample Number	^{238}U (ppb)	^{232}Th (ppt)	^{230}Th / ^{232}Th (atomic x10^{-6})	d^{234}U* (measured)	^{230}Th / ^{238}U (activity)	^{230}Th Age (yr) (uncorrected)	^{230}Th Age (yr) (corrected)	d^{234}U$_{Initial}$ ** (corrected)	^{230}Th Age (yr CE)
OJ-14a	1135.6 ±1.1	7859 ±157	18 ±1	1063.9 ±2.5	0.0077 ±0.0002	408 ±12	311 ±70	1065 ±2	1708 ±70
OJ-14b	949.9 ±1.2	6103 ±122	17 ±1	1066.8 ±3.2	0.0067 ±0.0003	356 ±16	266 ±66	1068 ±3	1753 ±66

mined by U series dating (Table 1). 30 mg of carbonate was sampled using a microdrill in a continuous air flow chamber at the Pyrenean Institute of Ecology (IPE-CSIC, Jaca). The carbonate powder was processed in the Isotope Geochemistry Laboratory at University of Minnesota (USA), following the protocol described in Edwards *et al*. (1987).

Five main detrital deposits were selected along the cave for further investigations (D1, D2, D3, D4, D5). Grain-size analyses were carried out on four (D1, D2, D4 (3 samples), and D5) of these deposits located at different elevation from the cave entrance. Particle size distribution (Sand (>63 μm), Coarse Silt (63-16 μm), Fine Silt (16-2 μm), Clay (2-0.01 μm)) was obtained for 6 samples (200 mg) by laser diffraction using a Mastersizer 2000 equipment at the IPE-CSIC Laboratory (Table 2). Sample (200 mg) pre-treatment includes disassembling, homogenization and removal of organic matter before scattering (McManus, 1988).

4. Results

4.1. Current hydrological observations

The cave entrance (spring) is only active during rainy periods or singular intense rainfalls. Once active, the water flow may persist for more than a month. After rainy periods, high-water marks are typically observed in the cave, indicating that the water can rise

Table 2: Particle size distribution of selected samples.
Tabla 2: Distribución del tamaño de partícula de las muestras seleccionadas.

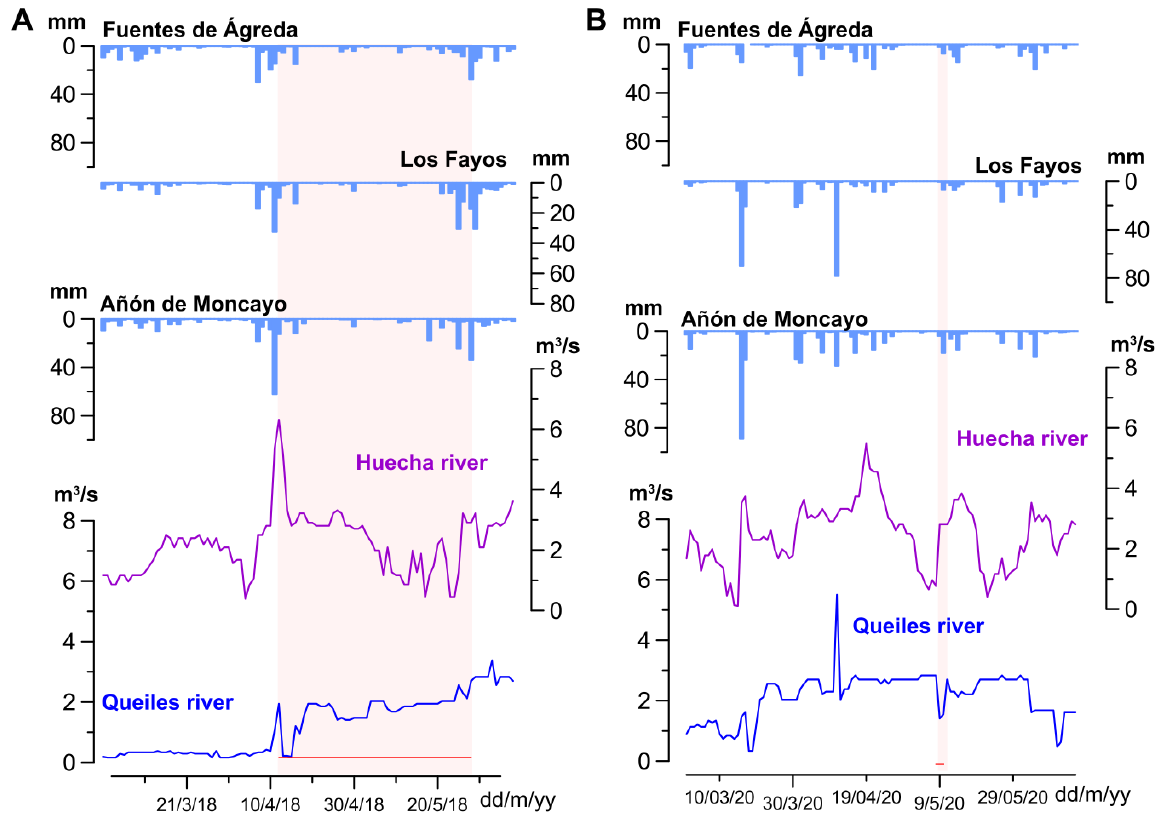| Deposit	Name	Clay (%) 0.01 μm - 2 μm	Fine silt (%) 2 μm - 16 μm	Coarse silt (%) 16 μm - 63 μm	Sand (%) >63 μm
D1	D1	4.7	25.4	21.8	48.2
D2	D2	6.4	33.8	43.7	16.0
D4	D4.1	4.2	19.7	50.3	25.8
D4	D4.2	3.3	12.9	51.3	32.4
D4	D4.3	4.2	18.5	51.9	25.4
D5	D5	5.9	24.8	51.1	18.2

Figure 2: Rainfall record at the pluviometers surrounding the Moncayo Massif, the response of Huecha and Queiles rivers and the periods when the spring was active (red vertical bars) between March and May 2018 (A) and 2020 (B).

Figura 2: Registro de las precipitaciones en los alrededores del Moncayo, las respuestas de los ríos Huecha y Queiles, y los periodos cuando la surgencia estaba activa (barras verticales rojas) para los eventos de marzo a mayo de 2018 (A) y de 2020 (B).

several meters, inundating areas that are not usually saturated with water. Below, we describe the weather conditions of two periods when the spring was active: March to May of 2018 and 2020.

The spatial distribution of rainfall over the Moncayo Massif varies from one event to another (Fig. 2A, B). For the first period, rainfalls of 20, 35, 60 mm were recorded in the pluviometer-network around Moncayo on April 11th 2018 (Fig. 2A). The highest rainfall amount was recorded in Añón de Moncayo (60 mm, 7.5 km to NW of the OdV cave). The day after the rainfall, we checked the spring and it was active. Several small landslides affected the road to access the cave and water emerged in several points of the slopes next

upstream to the cave entrance. A month later (15-05-2018), the spring was still active, although the flow decreased significantly. During that month, only minor rainfalls were recorded (Fig 2A). Huecha and Queiles rivers showed a fast and synchronous response to that rainfall episode.

For the second period, two rainfall events were investigated. On March 15th 2020, 89 mm of rainfall were recorded in Añón de Moncayo (Fig. 2B). Unfortunately, the spring could not be checked due to the lockdown situation caused by the COVID-19 pandemic. The second intense rainfall event, took place on May 9th 2020. This event was characterized by an intense and persistent rainfall that affected the area between Peñas de Herrera and the
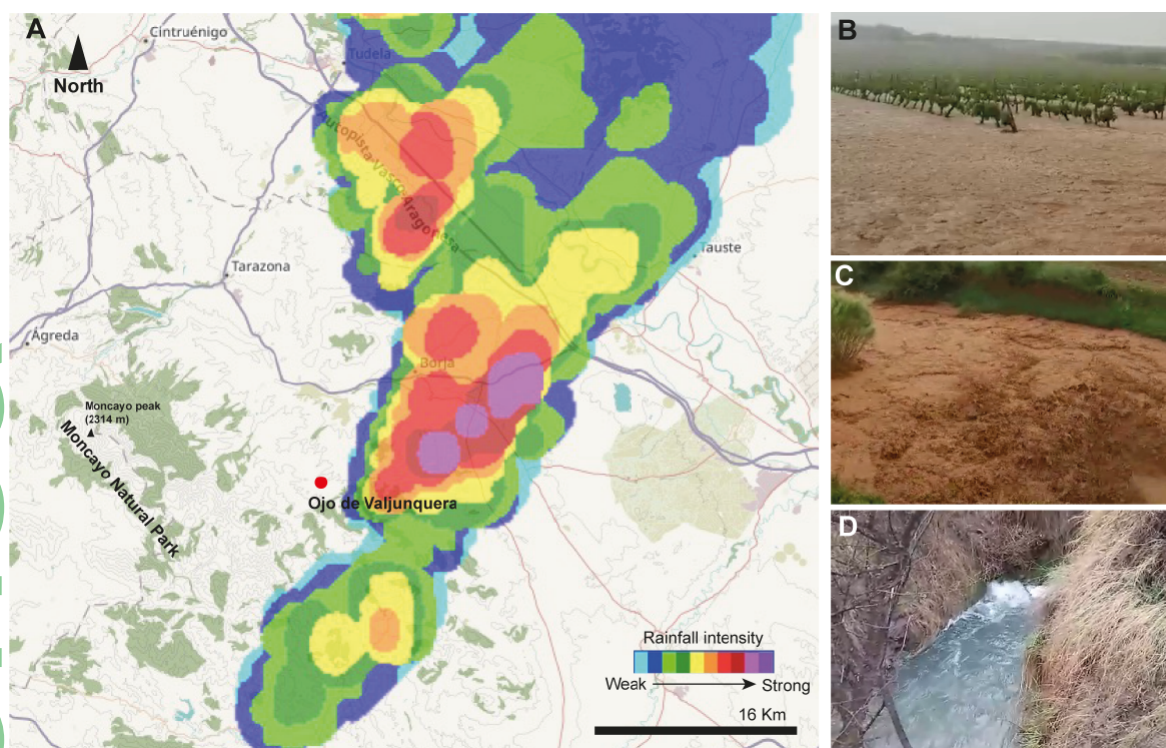
Figure 3. (A) Rainfall intensity map during May 9th 2020 at 17:10 hours. Modified from www.rain-alarm.com. (B) Vineyards flooded during the 2020 event. (C) View of Huecha river after the rainfall event. (D) Entrance of Ojo de Valjunquera after the extreme rainfall event.

Figura 3. (A) Mapa de la intensidad de la lluvia durante el evento del 9 de mayo de 2020 a las 17:10 horas. Modificado de www.rain-alarm.com. (B) Viñedos inundados durante el evento. (C) Vista del río Huecha tras el evento de lluvia. (D) Entrada del Ojo de Valjunquera tras el evento de lluvia extremo.

lower reach of Huecha River (Fig. 3A). Only small rainfall amounts (5 mm, Los Fayos, 20 mm in Añón de Moncayo) were recorded at the pluviometers, indicating that the event had a local extent and did not reach other areas in the region. Unfortunately, there is no record of the amount of rainfall during that extreme event in the immediate surrounding of the cave. During that event, some areas were flooded causing damages to the crops. The Huecha River responded promptly and the OdV spring flow was activated (Fig. 3B, C, D).

4.2. Geomorphological characteristic of the Ojo de Valjunquera cave

The OdV cave presents a longitudinal development of ~1033 m with two speleogenetic levels. The lower level is hydrologically active and feeds an ephemeral spring (the cave entrance). Six successive siphons lead to the end of this lower cave level (Fig. 4). While the first siphons can be easily passed, the last three require cave diving techniques, although siphon 4 may be sporadically accessible during droughts. Nevertheless, a series of shafts and ramps connect with the fossil upper level at a mean elevation of +11 m with respect to the cave entrance. After ~650 m both levels connect to form a single cave passage.

The galleries present circular sections, sub-horizontal notches, and well-developed scallops (Fig. 4). The cave sections are ~4-6 m in diameter with local constrictions (~0.5 m) (Fig. 4). Although the cave does not present a great speleothem development, certain
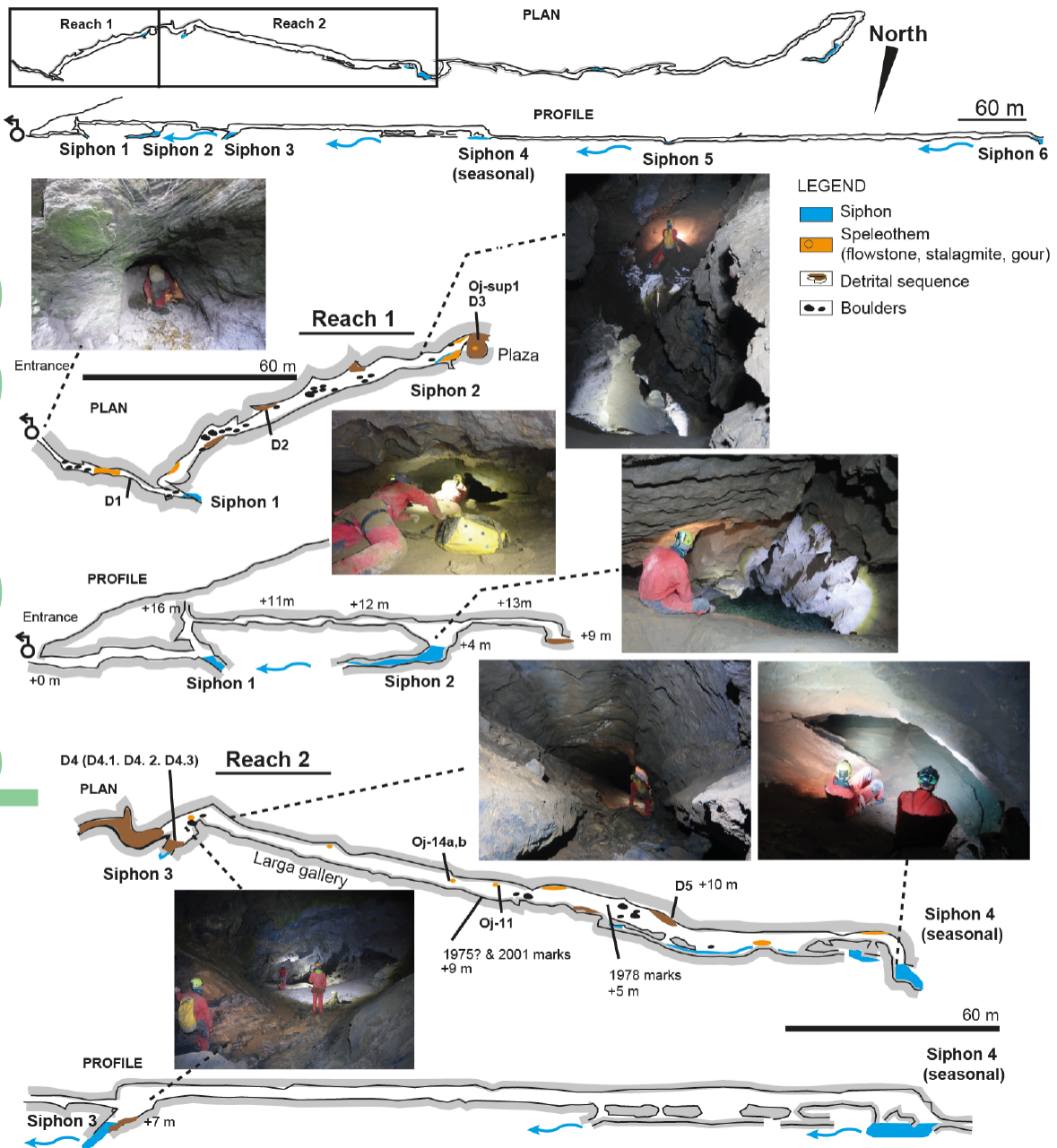
Figure 4. Cave topography modified from Gisbert and Pastor (2006) and approximate location of the main cave deposits and selected samples. Reach 1 and 2 represent the first ~ 650 m of the cave.

Figura 4. Topografía de la cavidad modificada de Gisbert y Pastor (2006) y localización aproximada de los principales depósitos de la cueva y de las muestras seleccionadas. Los tramos 1 y 2 representan, aproximadamente, los primeros 650 m de cueva.

Figure 5. (A) Stalagmites, columns, stalactites and flags covered by a fine coat of mud. (B) Modern-looking stalagmites growing over a centimetric sand layer in *Larga* gallery. (C) Block chaos at the beginning of the upper level. (D) Detrital deposit located in a blind area. (E) Deposit D1 in the lower gallery. (F) Example of four sand-clay sequences in deposit D4. (G) General aspect of deposit D5 and four cm-sequences recognized. (H) One of the signatures (marks) produced by cavers in the lower cave level. White arrows indicate signs of sediment remobilization (mud drops) after a flood.

Figura 5. (A) Estalagmitas, columnas, estalactitas y banderas cubiertas por una fina capa de barro. (B) Estalagmitas de aspecto reciente creciendo sobre una capa centimétrica de arena en la galería Larga. (C) Caos de bloques al comienzo del nivel superior. (D) Depósito detrítico localizado en una pequeña área ciega. (E) Depósito D1, localizado en la galería inferior. (F) Ejemplo de 4 secuencias de arena-arcilla del depósito D4. (G) Aspecto general del depósito D5 y cuatro secuencias poco claras de limo reconocidas. (H) Una de las firmas realizada por personas que entran en la cueva que han sido localizadas en el nivel inferior de la cueva. Las flechas blancas indican signos de removilización de sedimentos (gotas de barro) después de una inundación.

sectors are ornamented (Fig. 5A, B). Clastic accumulations represent the dominant deposits. Block accumulations produced by gravitational processes, dominate in the first meters of the upper gallery (Fig. 4, 5C). Thin cm-dm sandy deposits are coating the chaos of blocks and in blind sectors from the upper gallery (Fig. 5D). Detrital sediments also cover the cave-walls, ceilings, as well as speleothems surfaces (Fig. 5A). These sediments present a high amount of tiny shiny spots when they are under direct light which could relate to the presence of sheet silicates (phyllosilicates). Modern-looking stalagmites cover detrital sediments at different locations along the cave (Fig. 5B).

4.3. Cave deposits: distribution, arrangement and features

4.3.1. Detrital deposits

Five detrital sediment units were recognised. Grain size distribution of selected samples appear in Figure 6. Among those, D1 is highlighted due to its location in the lower gallery close to the entrance (Fig. 5E). The D1 deposit covers the walls and the cave ceiling suggesting that the cave outlet was completely blocked by sediments in the past. The se-

quence is formed by 150 cm of yellow sandy-silty sediments (Fig. 5E, Fig. 6, Table 2) with small layers of cm-sized gravels observed at the top. In the upper gallery, four detrital deposits (D2, D3, D4, D5) were described. The grain-size of deposits D1, D2, D4 and D5 (Table 2) shows a dominance of coarse silt (45% mean), followed by fine silt (22.5 % mean), sand (27.7 % mean) and clay (4.8 % mean). Samples D1 and D4.1, 4.2, 4.3 (Table 2) located at lower and intermediate cave elevations contain a higher percentage of sand particles. On the contrary, those samples located at higher cave positions (10-11 m; e.g. D2 and D5) (Table 3) contain the lowest percentage of sand and the highest amount of silt and clay. The D3 and D4 detrital deposits present the largest thickness of sediments. The main sedimentological features of these are summarized below:

— D3 (120 cm). The deposit is filling the bottom of a small shaft (*Plaza* sector). In general, the deposit is formed by rhythmic sand and silt layers (cm to mm in thickness) (Fig. 5F). At the bottom of the deposit, the sediments are accommodated to the cave topography, and rest horizontal towards the middle stretch of the sequence. Erosive bases as well as flame structures and mud clasts are observed along the depo-

Table 3: Meters of elevation of selected deposits and marks from the cave entrance.

Tabla 3: Elevación de los depósitos estudiados (en metros) y marcas seleccionadas, desde la entrada de la cueva.

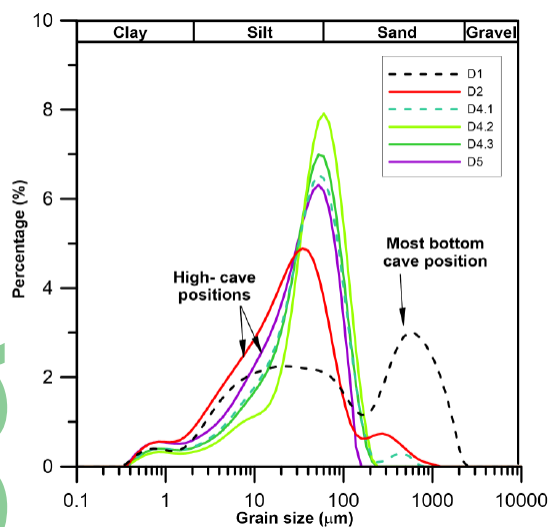| Deposit	Name	Elevation from entrance (m)
Stalagmite	Oj-11	~9
Stalagmite	Oj-14a	~9
Stalagmite	Oj-14b	~9
Stalagmite	Oj-sup1	~9
Clastic	D1	~2
Clastic	D2	~11
Clastic	D3	~9
Clastic	D4	~7
Clastic	D5	~10
Marks	1975? - 2001	~9
Marks	1978, BISA 85	~8

Figure 6. Grain size distribution (clay, silt, sand, gravel) of the percentage in volume of every grain-size class (assuming all spherical particles) in the selected samples.

Figura 6. Distribución del tamaño de grano (arcilla, limo, arena, grava) del porcentaje en volumen de cada clase de tamaño de grano (asumiendo todas las partículas esféricas) en las muestras seleccionadas.

sit. It is worth noting the presence of *in-situ* and broken stalagmites towards the top of the sequence. Levels of hard nodules are developed at the upper 40-20 cm. At the top of the sequence, a high concentration of mud clast occurs, covered by modern-looking stalagmites (OJ-sup1, Fig. 7).

— D4 (170 cm). The deposit covers the floor of the gallery that connects with siphon 3. In general, the deposit presents a more homogeneous character (Fig.5G) than deposit D1. The sediments comprise coarse silts and sands, with low amount of clays (Table 2). At the bottom, the deposit is dominated by flaser bedding. Towards the top, several sequences with decreasing grain size (Fig. 5G) and levels rich in carbonate nodules were recognized.

At the end of *Larga* gallery, several etchings made by cavers (e.g. dates) were identified. These marks were performed at different elevations over sandy/clayey deposits that
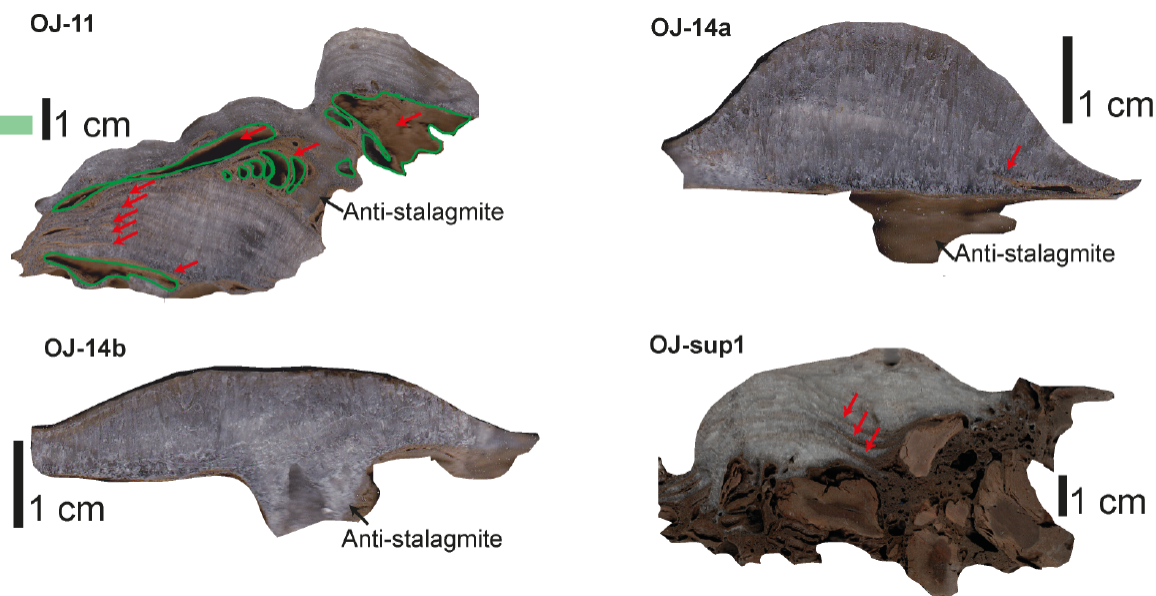

Figure 7. Selected stalagmites and visible detrital layers. Red arrows indicate detrital layers recognised at eye scale. Green lines represent washed off detrital layers during stalagmite sawing.

Figura 7. Estalagmitas seleccionadas y capas detríticas visibles. Las flechas rojas indican las capas detríticas reconocibles a escala de visu. Las líneas verdes representan capas detríticas vaciadas durante el corte de la estalagmita.

coat the gallery (Fig. 5H, Table 3). The prints present relative deep grooves (2-5 mm). The signatures (I-XI-78, BISA 29-11-85) located in a low position (8 m) show signs of reworking such as mudslides and mud drops (Fig. 5H). On the other hand, the marks located in higher positions (1975?[1] and 2001, 9 m) do not show evidence of any kind of clastic deposition over the grooves or degradation after they were done.

4.3.2. Speleothems

Speleothem formations comprise stalagmites, columns, stalactites and flags (Fig. 5A). These are located at different elevations along the upper cave level. Gours and microgours dominate in the lower level while carbonate rafts observed in the siphons illustrate the water saturation in carbonate. The selected stalagmites (Oj-11, Oj-14a, Oj-14b and OJ-sup1) were collected from the *Larga* gallery and *Plaza* sector, at an elevation of ~9 m with respect to the entrance (Fig. 4, Table 3). The stalagmite Oj-11 is 7 cm long (Fig. 7). In section, the sample shows translucent calcite and well defined fine detrital layers at the bottom, while four empty layers indicate the presence of sand that was washed off during the sample sawing. The samples Oj-14a (20 mm) and OJ-14b (11 mm) were twin stalagmites that grew over a detrital layer that covers the *Larga* gallery (Fig. 5B, 7). Both of them show anti-stalagmites (cylindrical shape structures) formed by the impact of drips over a non-consolidated sandy material. A fine sand layer is visible at ~16 mm from the top of sample Oj-14a (Fig. 7). Both stalagmites are currently growing, as shown by the carbonate precipitation over a glass slab. The ^{230}Th ages (Table 1) indicate that the speleothem started growing at 1708±70 CE and 1753±66 CE for Oj-14a and OJ-14b, respectively (Table 1). A simple linear age model between the top and bottom ages suggests growth rates of 64 μm a^{-1} and 41 μm a^{-1} for Oj-14a and OJ-14b, respectively. Finally, the stalagmite OJ-sup1

_____
1   Due to the degradation it is not clear to identify the last number of the year.

is 30 mm long and was recovered from the top of the detrital sequence D3, located in the *Plaza* sector (Fig. 4, 7). The stalagmite shows three distinct detrital layers at ~20, 23 and 27 mm from the top (Fig. 7).

5. Discussion

5.1. Grain size vs elevation of detrital sequences and origin of the material

The position of the different detrital sequences along with their grain-size composition provides evidence of water levels and flood intensity in the cave. The grain-size analyses show that D1, located 2 m upstream of the spring, has the highest amount of sand (48.2%) and gravels (do not considered for granulometric analysis), while the highest samples taken from deposits D2 (+11 m) and D5 (+10m) show the lowest proportions of sand (16% and 18.2% respectively). A strong negative correlation (R^2=0.94) between the elevation and the percentage of sand of the selected deposits along the cave (~3.5% m^{-1}) is noted. On the contrary, the sum of coarse and fine silt shows a positive correlation (R^2=0.92) with an increasing proportion at higher elevation (Fig. 8). A lower correlation is observed for the clay fraction (R^2=0.31), although it dominates in the highest deposits (D2, D5). This low correlation is probably due to the relative high presence of clay in D1. The decrease in coarse material with elevation is likely related to the energy of the water flow during a flood event in the cave. Thus, the coarse material is deposited in the lower sectors, while only silt and clay sized sediments reach the upper parts. Based on similar observations, González-Lemos *et al*. (2015a) indicated that only the largest floods (in terms of intensity) can transport coarse material towards the elevated areas. These authors distinguished between minor and major floods recorded in stalagmites. Major floods usually deposit continuous detrital layers (>0.1 mm) when the discharge slowly recedes to the base flow. On the other hand, minor floods are represented by thinner and
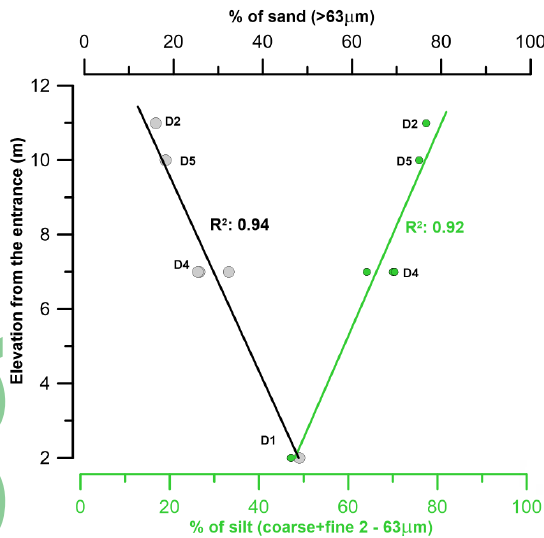
En prensa

In press

Figure 8. Relation between the elevation of selected deposits and their grain-size classes.

Figura 8. Relación entre la elevación de las muestras seleccionadas respecto a la entrada de la cueva y la granulometría.

discontinuous layers. In fact, the stalagmite Oj-11 shows clearly two types of detrital layers. The first comprises, four thick layers, which could correspond to large floods, while the second type comprises only thin layers hinting towards smaller floods.

5.2. Sedimentary effects in the cave of an intense rainfall

Our observations suggest that the intense rainfalls in the area (> 60 mm) lead to an activation of the spring and subsequent increase of cave water levels. The cave acts as an overflow of the karst system of the springs located downstream. We identified some watermarks nearby the siphons. For example, the caver´s marks located at 8 m elevation show clear evidence of reworking processes thus confirming that the water level reached this elevation. However, the etching "1975? – 2001" (9 m) remains intact and without signs degradation by water since it was produced suggesting the lack of a large flood since year 2001. Another interesting observation is the modification of the trenches we performed for the sedimentological description. The trenches

D3 and D4 were dug between December 2019 and March 7th 2020. After the lockdown due to the COVID-19 pandemic, we went back to the cave in July 2020 finding that the trench excavated in D4 was completely filled with sediments. Similarly, part of the trench in D3 collapsed and the sediment pile associated with the digging (~1m thick) showed signs of reworking. Eventually, an informative panel left to explain the ongoing scientific work was covered by a fine layer of mud. Similar evidences of sediment remobilization in caves were observed elsewhere (Bättig and Wildberger, 2007; van Gundy and White, 2009; González-Lemos *et al.*, 2015a, 2015b).

Our observations indicate that water rises by up to ~4 m between the *Plaza* sector and siphon 3. Probably, this flooding corresponds to rainfalls produced on March 15th 2020 and/or May 9th 2020. Thus, the D3 detrital sequence, and speleothems within and over it (Oj-sup1), record rainfall events >60 mm, while the D4 located at a lower position records less intense events. These deposits comprise mainly slackwater facies formed by sandy-clayey sequences deposited as a suspended load in blind zones or upstream of narrow galleries (Bosch and White, 2007). Given the environment of deposition, the observed liquefaction-structures seem to be related to the density contrast and the pressure of the water column over the sediments during the flood event; a relation to seismic movements is less likely. Mud clasts within the sequence D3 were deposited by energetic flows that were able to rip-up dry clayey sediments coating the gallery bottom as well as broken stalagmites.

On the other hand, the hydraulic head rise associated with D2 and D5 sequences, which are located at the highest elevations, could be related to extreme rainfall events. At this point, we consider possible morphological changes of the cave section due to sedimentary infills. In fact, stratigraphic features within D1 sequence suggest that the sediments were able to block completely the cave outlet. Moreover, the rest of sand nodules observed along the *Larga* gallery as well as in elevated

positions close to D5 sequence, indicate the presence of past sediments in those areas. Thus, the blockage of the entrance gallery by sediments and the sediment accumulation in other cave sectors may introduce temporal changes in cave geometry likely affecting the hydraulic head rise (e.g Denniston and Luetscher, 2017). This situation would imply that also regular floods may have reached elevated areas. Therefore, an alternative hypothesis considers that detrital D2 and D5 sequences could have been deposited under a blocked spring mode, and not necessarily reflecting extreme events. On the other hand, even if we have observed that the water level rises by approximately 9 m with respect to the cave entrance in the *Plaza* sector, the signature marks ("1975? – 2001" at 9 m in height) located towards the end of the reach 2 in the cave do not present signs of reworking. This is probably related to the different diameters of the cave section in the siphons along the cave indicating the importance of detailed cave geomorphological studies to really understand the effects of flood events.

The source of detrital material is most likely from the insoluble residue generated in the cave due to limestone dissolution (autochthonous) and sediments introduced into the cave by runoff (allochthonous) (Bosch and White, 2007). The hydrological context of Moncayo Massif, with the capture of creeks by the limestone units in contact with the Talamantes fault, suggests that siliciclastic material from the Buntsandstein formation is the main sediment source, explaining the high content in shiny minerals observed in the cave detrital deposits. Thus, the hydrological catchment area likely corresponds to the creeks nearby Talamantes or Añón de Moncayo which drain the Peñas de Herrera sector.

5.3. Do stalagmites serve as a good record of historical floods?

The ^{230}Th ages from the bases of twin stalagmites OJ-14a and Oj-14b point out that the detrital layer over which they grew is older than 1708±70 CE. In this case, the low consolidation of that detrital layer as well as the anti-stalagmite formed, indicate an immediately carbonate precipitation after the sedimentation of the detrital layer, and therefore, it should not be much older than the onset of carbonate precipitation. Considering a simple age model, the detrital layer observed at ~16 mm from the top of the stalagmite Oj-14a indicates a flood event which would have occurred approximately on the year 1770 CE. Therefore, the sand layer located below the stalagmite and the layer hosted inside may correspond to two important floods in the region. Coherently, among the two most important floods in the Queiles River we highlight the ones that took place on October 14th 1709, and on October 2nd 1755. The first flood is known as "*La noche de la ruina*" (The night of the ruin) (Diario de Navarra, 2009) since, during that night, an important flood of the Queiles and Mediavilla rivers devastated part of the city of Tudela, probably associated with heavy rainfalls in Moncayo and Cierzo mountains. This flood provoked severe damages in Tudela, with defences of the Succession War (1700-1714) being destructed. Approximately 300 houses were destroyed as well as the bridges of both rivers. The days after the flood, a total of 100 bodies were found within the ruins.

Given the rainfall distribution during heavy rainfall events and considering the uncertainties on the stalagmite chronology, we suggest that the centimetre non-consolidated detrital layer found just below the stalagmite could correspond to that extreme event of October 14th 1709. In addition, the detrital layer observed at 16 mm depth could possibly relate with the extreme flood that occurred in October 2nd 1755. After those events, no more floods were intense enough to reach the stalagmite site, as deduced from our visual observations. That is also in agreement with the absence of reworking evidences of the 2001 marks located at a similar elevation in the gallery.

In the other selected stalagmites some flood layers were also identified. Thus, the fine layers in Oj-11 would indicate low energy floods

during a short time interval, while the thicker ones should be related to high amount of sediments transported during energetic floods. In the case of Oj-Sup1, the sand layers would represent flood events major to 60 mm in the area, similar to those interpreted for D4 deposit.

6. Conclusions and future remarks

A first recognition of the Ojo de Valjunquera cave based on geomorphological, topographical, hydrogeological, and chronological analyses, allows us evaluating the suitability of this cave for the study of past floods. We summarize our main findings below:

— The cave presents two speleogenetic levels: the lower one, which is hydrologically active, comprises six siphoning areas; and, an upper fossil level where speleothems and detrital sequences dominate. Both levels are connected by shafts and ramps, which favour the rise of water during flooding.

— Detrital sequences show decreasing percentages of sand and an increase in silt with the elevation of the deposits with respect to the cave entrance. This change in grain-size is related to the slackwater conditions (low energy) during flood episodes. The stalagmites show two types of detrital layers. Thin layers are interpreted to correspond with low energy floods occurring in a short time interval, and the thicker ones are likely related to large, very energetic flooding transporting a high amount of sediments. The main source of clastic sediments in the cave corresponds to the siliciclastic materials from the Buntsandstein outcroping at the stream headwaters.

— The rainfall record indicates, in general, a homogeneous precipitation distribution in the Moncayo area. The spring is active with rainfall episodes larger than 60 mm and it can be active for more than a month. On the other hand, the cave flow also responds to intense and very local rainfall events. Thus, the flood record in the stalagmites and the detrital sequen-

ces may represent either extreme local and/or regional rainfalls. This hypothesis is exemplified by the case of two historical floods that were recorded in the cave stalagmite record. The replication of these flood events in other stalagmites will require further efforts in the nearby future.

— The morphosedimentary and geomorphological observations indicate that water level reached to the cave ceiling in the past. Current observations point out that in some sectors the water level rose by ~9 m with respect to the elevation of the cave entrance. However, the sectors before and after the siphons have different responses depending on conduit geometry of the lower gallery. In addition, the cave outlet could have been completely blocked in the past due to massive remobilization of cave sediments. Eventually, some sectors provide evidence of sedimentary infills that later disappeared. Therefore, the highest elevation of the detrital sequences and the floods recorded in the stalagmites may not necessarily represent the most extreme events but appear as a consequence of modified cave morphology. Future work must be focused on the chronology of the sediments that block the cave outlet, to interpret correctly the flood layers recorded in the speleothems and detrital deposits.

— This study carried out in the Ojo de Valjunquera indicates the high potential of this cave for paleoflood reconstruction combining speleothems and detrital deposits. Among the main advantages, it is worth to highlight five points: 1) the cave conduit configuration by two simple galleries connected by shafts; 2) the presence of detrital and chemical deposits and their relative high positions with respect to the spring; 3) the internal structure of the stalagmites formed by clean carbonate clearly alternating with detrital layers; 4) enough amount of uranium and relatively low concentrations of detrital thorium to guarantee a good chronological framework to study the Holocene period and 5)

the unique response of the water level to intense local/regional rainfalls.

— Future work will focus on the implementation of hydraulic model based on the 3D-structure of the conduit network, discharge measurements, as well as calibration data from water-level monitoring (hydraulic head) to quantify the magnitude of past floods recorded in stalagmites and detrital sequences.

References

Aranbarri, J., Bartolomé, M., Alcolea, M., Sancho, C., Celant, A., González-Sampériz, P., Arenas, C., Magri, D., Rodríguez-Lázaro, J. (2016). Palaeobotanical insights from Early-Mid Holocene fluvial tufas in the Moncayo Natural Park (Iberian Range, NE Spain): Regional correlations and biogeographic implications. *Review of Palaeobotany and Palynology,* 234, 31-43. https://doi.org/10.1016/j.revpalbo.2016.08.006

Arnaud, F. (2005). Discriminating bio-induced and detrital sedimentary processes from particle size distribution of carbonates and non-carbonates in hard water lake sediments. *Journal of Paleolimnology,* 34 (4), 519-526. https://doi.org/10.1007/s10933-005-6787-1

Bättig, G., Wildberger, A. (2007). Ein Vergleich des Hölloch-Hochwassers vom August 2005 mit seinen Vorgängern. *Stalactite,* 57 (1), 26-34.

Benito, G., Thorndycraft, V.R., Rico, M., Sánchez-Moya, Y., Sopeña, A. (2008). Palaeoflood and floodplain records from Spain: Evidence for long-term climate variability and environmental changes*. Geomorphology*, 101 (1-2), 68-77. https://doi.org/10.1016/j.geomorph.2008.05.020

Benito, G., Macklin, M.G., Panin, A., Rossato, S., Fontana, A., Jones, A.F., Machado, M.J., Matlakhova, E., Mozzi, P., Zielhofer, C. (2015). Recurring flood distribution patterns related to short-term Holocene climatic variability. *Scientific Reports,* 5, 16398. https://doi.org/10.1038/srep16398

Blöschl, G., Kiss, A., Viglione, A., Barriendos, M., Böhm, O., Brázdil, R., Coeur, D., Demarée, G., Llasat, M.C., Macdonald, N., Retsö, D., Roald, L., Schmocker-Fackel, P., Amorim, I., Bělínová, M., Benito, G., Bertolin, C., Camuffo, D., Cornel, D., Doktor, R., Elleder, L., Enzi, S., Garcia, J.C., Glaser, R., Hall, J., Haslinger, K., Hofstätter, M., Komma, J., Limanówka, D., Lun, D., Panin, A., Parajka, J., Petrić, H., Rodrigo, F.S., Rohr, C., Schönbein, J., Schulte, L., Silva, L.P., Toonen, W.H.J., Valent, P., Waser, J., Wetter, O. (2020). Current European flood-rich period exceptional compared with past 500 years. *Nature*, 583, 560-566. https://doi.org/10.1038/s41586-020-2478-3

Bosch, R.F., White, W.B. (2004). Lithofacies And Transport Of Clastic Sediments In Karstic Aquifers. In: Sasowsky, I.D., Mylroie, J. (Eds.), *Studies of Cave Sediments: Physical and Chemical Records of Paleoclimate*. Springer Netherlands, Dordrecht, 1-22. https://doi.org/10.1007/978-1-4020-5766-3_1

CHEBRO (2006). INFORME PIEZÓMETRO DE AMBEL 3 "VALJUNQUERA": 09.602.019. Proyecto de Construcción de Sondeos e Instalación de la Red Oficial de Control de Aguas Subterráneas de la Cuenca del Ebro 2ª fase. 40 pp.

Cheng, H., Lawrence Edwards, R., Shen, C.-C., Polyak, V.J., Asmerom, Y., Woodhead, J., Hellstrom, J., Wang, Y., Kong, X., Spötl, C., Wang, X., Calvin Alexander, E. (2013). Improvements in 230Th dating, [230]Th and [234]U half-life values, and U-Th isotopic measurements by multi-collector inductively coupled plasma mass spec-

trometry. *Earth and Planetary Science Letters,* 371-372, 82-91. https://doi.org/10.1016/j.epsl.2013.04.006

Corella, J.P., Benito, G., Rodriguez-Lloveras, X., Brauer, A., Valero-Garcés, B.L. (2014). Annually-resolved lake record of extreme hydro-meteorological events since AD 1347 in NE Iberian Peninsula. *Quaternary Science Reviews*, 93, 77-90. https://doi.org/10.1016/j.quascirev.2014.03.020

Corella, J.P., Valero-Garcés, B.L., Vicente- Serrano, S.M., Brauer, A., Benito, G. (2016). Three millennia of heavy rainfalls in Western Mediterranean: frequency, seasonality and atmospheric drivers. *Scientific Reports,* 6, 38206 https://doi.org/10.1038/srep38206

Cuadrat, J.M., Saz Sánchez, M.A., Vicente Serrano, S.M. (2008). Atlas climático de Aragón. Departamento de Medio Ambiente. Gobierno de Aragón, 291 p.

Denniston, R.F., Luetscher, M. (2017). Speleothems as high-resolution paleoflood archives. *Quaternary Science Reviews*, 170, 1-13. https://doi.org/10.1016/j.quascirev.2017.05.006

Denniston, R.F., Villarini, G., Gonzales, A.N., Polyak, V.J., Ummenhofer, C.C., Lachniet, M.S., Wanamaker, A.D., Humphreys, W.F., Woods, D., Cugley, J. (2015). Extreme rainfall activity in the Australian tropics reflects changes in the El Niño/Southern Oscillation over the last two millennia. PNAS *Proceedings of the National Academy of Sciences of the United States of America*, 112(15), 4576-4581. https://doi.org/10.1073/pnas.1422270112

Diario de Navarra (2009) 14 de octubre de 1709, La noche de la ruina. *Diario de Navarra*. https://www.diariodenavarra.es/20091014/tudela/14-octubre-1709-noche-ruina.html [Consulted on April 28th 2021].

Gázquez, F., Calaforra, J.M., Forti, P., Stoll, H., Ghaleb, B., Delgado-Huertas, A. (2014). Paleoflood events recorded by speleothems in caves. *Earth Surface Processes and Landforms* 39, 1345-1353. https://doi.org/10.1002/esp.3543

Gisbert, M., Pastor, M. (2006). Cuevas y simas de la provincia de Zaragoza. Centro de Espeleología de Aragón, 480 p.p

González-Lemos, S., Jiménez-Sánchez, M., Stoll, H.M. (2015a). Sediment transport during recent cave flooding events and characterization of speleothem archives of past flooding. *Geomorphology,* 228, 87-100. https://doi.org/10.1016/j.geomorph.2014.08.029

González-Lemos, S., Müller, W., Pisonero, J., Cheng, H., Edwards, R.L., Stoll, H.M. (2015b).

Holocene flood frequency reconstruction from speleothems in northern Spain. *Quaternary Science Reviews*, 127, 129-140. https://doi.org/10.1016/j.quascirev.2015.06.002

Jaffey, A.H., Flynn, K.F., Glendenin, L.E., Bentley, W.C., Essling, A.M. (1971). Precision Measurement of Half-Lives and Specific Activities of U^{235} and U^{238}. *Physical review C*, 4 (5), 1889-1906. https://doi.org/10.1103/PhysRevC.4.1889

Longares, L.A. (2004). El paisaje vegetal en el sector aragonés del Moncayo. In: Peña, J.L., Longares, L.A., Sánchez, M. (Eds.) *Geografía Física de Aragón. Aspectos generales y temáticos*. Universidad de Zaragoza e Institución Fernando el Católico, pp0. 187-197 [WWW Document].

McManus, J. (1988). Grain size determination and interpretation. In: Tucker, M.E. (Ed.), Techniques in Sedimentology. Blackwell, Oxford, 63-85.

San Román, J., Sánchez, J., Martínez, F.J. (1989). El drenaje subterráneo del macizo del Moncayo: aspectos hidrológicos e hidroquímicos. *Tvriaso*, IX, 203-224.

Sancho, C., Arenas, C., Vázquez-Urbez, M., Pardo, G., Lozano, M.V., Peña-Monné, J.L., Hellstrom, J., Ortiz, J.E., Osácar, M.C., Auqué, L., Torres, T. (2015). Climatic implications of the Quaternary fluvial tufa record in the NE Iberian Peninsula over the last 500 ka. *Quaternary Research*, 84, 398-414. https://doi.org/10.1016/j.yqres.2015.08.003

Thorndycraft, V.R., Benito, G. (2006). The Holocene fluvial chronology of Spain: evidence from a newly compiled radiocarbon database. *Quaternary Science Reviews*, 25, 223-234. https://doi.org/10.1016/j.quascirev.2005.07.003

van Gundy, J.J., White, W.B. (2009). Sediment flushing in Mystic Cave, West Virginia, USA, in response to the 1985 Potomac Valley flood. *International Journal of Speleology,* 38, 103-109. https://doi.org/10.5038/1827-806X.38.2.2

Wilhelm, B., Cánovas, J.A.B., Macdonald, N., Toonen, W.H.J., Baker, V., Barriendos, M., Benito, G., Brauer, A., Corella, J.P., Denniston, R., Glaser, R., Ionita, M., Kahle, M., Liu, T., Luetscher, M., Macklin, M., Mudelsee, M., Munoz, S., Schulte, L., George, S.S., Stoffel, M., Wetter, O. (2019). Interpreting historical, botanical, and geological evidence to aid preparations for future floods. *WIREs Water,* 6, e1318. https://doi.org/10.1002/wat2.1318